Effects of Peptides Derived from Terminal Modifications of the Aβ Central Hydrophobic Core on Aβ Fibrillization

Cyrus K. Bett,[†] Wilson K. Serem,[†] Krystal R. Fontenot,[†] Robert P. Hammer,[‡] and Jayne C. Garno*,[†]

[†]Department of Chemistry, Louisiana State University, Baton Rouge, Louisiana 70803, and [‡]New England Peptide LLC, 65 Zub Lane, Gardner, Massachusetts 01440

Abstract

Considerable research effort has focused on the discovery of mitigators that block the toxicity of the β-amyloid peptide (Aβ) by targeting a specific step involved in Aβ fibrillogenesis and subsequent aggregation. Given that aggregation intermediates are hypothesized to be responsible for Aβ toxicity, such compounds could likely prevent or mitigate aggregation, or alternatively cause further association of toxic oligomers into larger nontoxic aggregates. Herein we investigate the effect of modifications of the KLVFF hydrophobic core of Aβ by replacing N- and C-terminal groups with various polar moieties. Several of these terminal modifications were found to disrupt the formation of amyloid fibrils and in some cases induced the disassembly of preformed fibrils. Significantly, mitigators that incorporate MiniPEG polar groups were found to be effective against $A\beta_{1-40}$ fibrilligonesis. Previously, we have shown that mitigators incorporating alpha,alpha-disubstituted amino acids (ααAAs) were effective in disrupting fibril formation as well as inducing fibril disassembly. In this work, we further disclose that the number of polar residues (six) and ααAAs (three) in the original mitigator can be reduced without dramatically changing the ability to disrupt $A\beta_{1-40}$ fibrillization in vitro.

Keywords: Amyloid peptide (Aβ), fibrils, spherical structures, mitigators, assembly, disassembly

A standing hypothesis associated with Alzheimer's disease (AD) is that aggregation of monomeric β-amyloid (Aβ) fibrils into the neurotoxic misfolded forms is the key event associated with the disease pathogenesis (*1*−*3*). Recently, extensive investigation of the aggregation pathway reveals that oligomeric assemblies and not mature fibrils are responsible for Aβ neurotoxicity (*4*−*9*). Several approaches have been designed to target the Aβ assembly process in an effort to reduce toxic species in the brain. Peptide-based approaches in particular are increasingly becoming a vital constituent of new therapeutics because of their high specificity and low toxicity as compared to that of small organic molecules (*10*).

Several groups have developed amyloid aggregation mitigating peptides (AAMPs) based on designed changes to the $A\beta_{16-20}$ central hydrophobic core, KLVFF fragment, which Tjenberg (*11*, *12*) showed to be critical for Aβ self-assembly and self-recognition. To the KLVFF core, a "disrupter" group is added that either solubilizes inhibitor-Aβ aggregates or blocks further addition of β-sheets through hydrogen bonding. Disrupters that have been added to peptides can be classified as N- or C-terminal modifications (*13*), conformationally constrained amino acids (*14*), peptide backbone modifications (*15*), or as the use of D-amino acids (*16*).

An example for C-terminal modifications was the addition of oligolysine chains to the C-terminus of the KLVFF motif to design the peptide KLVFFKKKKKK, which was shown to enhance the rate of $A\beta_{1-40}$ aggregation into fibrils and thereby prevent toxicity against PC12 cells (*13*, *17*). Also, the rate of Aβ assembly into fibrils was shown to depend on the number of lysine groups present in the mitigator. Several modifications of the peptide backbone for the KLVFF binding motif have been reported. These include the replacement of amide hydrogen with methyl groups (*15*, *18*) and replacement of the amide bond with either an ester bond (*19*) or isostructural E-olefin (*20*). These modifications were designed to block the proliferation of hydrogen-bonding between β-sheets that is necessary for Aβ fibrillization. Peptides derived from these modifications were found to disrupt $A\beta_{1-40}$ fibril formation and to disassemble preformed fibrils. For instance, N-methylated peptide Aβ16−22m (*15*) and esterificated Aβ16−20e (*19*) disrupted fibril formation and caused the disassembly of preformed fibrils. Also, it was demonstrated that mutations of the Phe19-Phe20 amide bond of $A\beta_{1-40}$ with an E-olefin bond exclusively produced spherical aggregates and that fibrillization was not detected despite incubation periods of up to 6 weeks (*20*, *21*).

Received Date: September 24, 2009
Accepted Date: August 5, 2010
Published on Web Date: August 26, 2010

DOI: 10.1021/cn900019r | *ACS Chem. Neurosci.* (2010), *1*, 661–678

Conformationally constrained peptides have been shown to be effective at disrupting Aβ fibril formation through unfavorable steric interactions. For instance, a β-sheet breaker peptide, iAβ5 containing one proline residue was shown to disrupt fibril formation, disassemble preformed fibrils, and protect against neurotoxicity (*22*). Our approach for this report involves replacing the hydrogen atom of the α-carbon of natural amino acid residues (to form alpha,alpha-disubstituted amino acids, ααAAs) in the KLVFF motif with an alkyl substituent. Thus, the conformational freedom of the peptide is restricted, and it is forced to adopt an extended conformation that is ideal for interaction with Aβ_{1-40} (*23*, *24*). Peptides in an extended conformation form two faces where one face is available for interaction with Aβ, while the other is sterically blocked, limiting β-sheet extensions required for amyloid fibril propagation.

Apart from blocking hydrogen bonding between β-sheets, incorporation of ααAAs within the KLVFF motif also increases the overall hydrophobicity of the mitigator peptide and in turn strengthens the hydrophobic interactions with the Aβ_{1-40} target. Polar groups are normally added to the highly hydrophobic ααAA-containing KLVFF core to increase the overall solubility of the peptide. Also, modification of the α-carbon helps to decrease susceptibility of the mitigator to proteolytic degradation, which ensures effective delivery of the inhibitor to the target organ during in vivo studies. In general, our design for mitigators combines the advantages of both C-terminal and α-carbon modification.

We have previously developed a mitigator peptide (AMY-1) with a C-terminal oligolysine chain (KDibgVDbgFDpgK$_6$) and a peptide (AMY-2) with an N-terminal oligolysine chain (K$_7$KDibgVDbgFDpg). Both mitigator peptides AMY-1 and AMY-2 disrupted fibril formation and formed spherical aggregates of different heights (*25*). We have shown that AMY-1 has the ability to reduce Aβ deposits when injected into the hippocampus of 14-month-old APP transgenic mice, a model of amyloid deposition (*26*). Although, AMY-1 showed tendencies to reduce Aβ deposits, it was toxic at high doses. We postulate that AMY-1 toxicity is due to either the overall charge from the six lysines or due to the size of the mitigator, which might hinder its movement across the brain barrier. Thus, the charge and molecular weight of the mitigator should be reduced for optimal use in vivo and improved systemic bioavailability. Incorporation of one or two ααAAs in the KLVFF binding motif was previously shown to be effective at disrupting Aβ_{1-40} fibrillization as compared to the original peptide (AAMP-1) with three ααAAs (*27*). Herein, the effects of forming Aβ fibrils in the presence of amyloid aggregating mitigating peptides (AAMPs) incorporating different polar solubilizing groups (C- or N-terminal) are studied in an effort to evaluate the effectiveness of reducing the overall charge of the mitigator. Also, the effects of ααAA-containing AAMPs with fewer polar groups as compared to those of the original mitigator AAMP-1 with six Lys are presented.

Peptide analogues modified with α-amino isobutyric acid (also called α-methyl alanine) have been shown to be more effective at inducing the disassembly of Aβ fibrils than either L-proline or D-amino acids in short model peptides (*28*, *29*). The restrictions imposed by α-methyl alanine or C$^{-\alpha}$-tetra-substituted-amino acid on conformational freedom are more severe than those of proline. Thus, mitigators containing bulky substituents (ααAAs) could be more effective at inducing β-sheet disassembly than peptides that incorporate proline. Simulation experiments have shown that N-methylated peptide Aβ16−22m interacts with the Aβ_{16-22} blocking β-sheet extension, preventing lateral association into layers, and more importantly blocking inhibitor intercalation for sequestering Aβ peptides. However, Aβ16−22m has also been to shown in vivo to increase Aβ deposition in the brain of APP transgenic mice, unlike our peptide AMY-1 which showed ability to reduce Aβ deposits. Our ααAAs are bulkier than either N-methylated or α-methyl alanine model peptide derivatives. Thus, we hypothesize that ααAA-AAMPs could be more effective at both disrupting fibril formation as well as inducing the disassembly of preformed fibrils.

Results and Discussion

Design of Peptides for Mitigating Aβ Aggregation

Initial work by Tjenberg identified the Aβ central hydrophobic core KLVFF as the key scaffold for designing disrupters of Aβ_{1-40} fibrillization (*11*, *12*). Disrupting elements have been strategically placed at various positions within the Aβ hydrophobic core that either solubilize the AAMP-Aβ aggregate (Lys or Arg) or block one hydrogen boding face inhibiting β-sheet extension or propagation as with N-Me amino acid or ester bonds. Thus, polar groups such as Arg, Lys, Glu, and PEG chains were added to increase the solubility of peptides. Certain mitigators incorporating these polar groups have been shown to be effective at disrupting fibril formation (*17*).

Surface plasmon resonance (SPR) was employed by Murphy and co-workers (*30*) to study the binding of variants related to KLVFF on immobilized Aβ_{10-35} fibrils (*12*). Variants with positively charged residues (KLVFFK$_n$) added to the C-terminus had higher affinities for immobilized Aβ_{10-35} fibrils than the KLVFF control, while negatively charged residues (KLVFFE$_n$) also placed on the C-terminus had a significantly lower

DOI: 10.1021/cn900019r | ACS Chem. Neurosci. (2010), 1, 661–678

binding affinity. In contrast, N-terminal addition of positively charged residues (K_nKLVFF) resulted in lower affinity. Binding affinity also is affected by additions of polar groups that do not precede the KLVFF region in the parent Aβ sequence. Therefore, amino acids (for example Gly) that are conformationally unrestricted can be used as a spacer between the KLVFF motif and solubilizing residues. Using Gly as a spacer between the mitigator KLVFF core and Arg residues (solubilizing agents) on both the C- and N-termini, Austen et al. designed the peptide RGKLVFFGR (*31*). This peptide was shown to be an effective disrupter of Aβ_{1-40} fibril formation and to prevent neurotoxicity toward human neuroblastoma SHSY5Y cells.

As part of our continuing work to design more effective ααAA-containing AAMPs (*14*), we employed similar strategies for placing spacers between the AAMP core KLVFF and the solubilizing groups. We have previously shown that AAMP-1 disrupted Aβ fibril formation (*25*). In vivo studies of AAMP-1 on APP transgenic mice displayed elevated toxicity at higher concentrations (*32*). The toxicity observed could be related to the six cationic lysines which also affect the delivery of drugs across the hydrophobic brain barrier during in vivo studies. Thus, positively and negatively charged polar amino acids as well as neutral polar groups such as MiniPEG were evaluated for effects on the morphology of resulting nanoparticles. Our goal was to reduce the overall charge of the original peptide (AAMP-1) without sacrificing the mitigator ability to disrupt fibril formation and induce disassembly of preformed fibrils.

Our design of mitigators is based on the much described Aβ central hydrophobic core. Solubilizing polar residues were added to this core, however, with a spacer in between them as previously described by Austen and co-workers (*31*). Several peptide mitigators (Table 1) were designed to probe the effect of various polar groups (positive, negative, or neutral) and/or substitution of natural amino acids with α,α-disubstituted amino acids on Aβ_{1-40} fibrillization. Peptide mitigator AAMP-11 described by Austen and coworkers was used as a control peptide. First, the effect of various polar groups on Aβ_{1-40} aggregation was investigated by designing mitigators where Arg (control peptide) is replaced with Lys (AAMP-12), Glu (AAMP-13), and MiniPEG (AAMP-14) (Table 1). Mitigator AAMP-15 allowed us to probe the effect of increasing the number of Arg in the chain to three on both the C-and N-terminus on Aβ fibrillogenesis. Peptide mitigators AAMP-16, AAMP-17, and AAMP-18 were designed to evaluate the effect of placing polar groups Arg, MiniPEG, and Lys, respectively, on only the C-terminus. The effect of placing polar groups on the N-terminus was evaluated using AAMP-19 with Arg added only to the N-terminus. We have previously shown that one, two, or three ααAAs incorporated in a mitigator sequence with six C-terminal lysines was efficient in disrupting the process of Aβ fibrillization (*27*, *33*). Thus, mitigators AAMP-20, AAMP-21, AAMP-22, AAMP-23, and AAMP-24 were designed to probe the effect of reducing both the number of ααAAs as well as lysines on Aβ fibrillization. We hypothesize that the addition of a spacer between the ααAA-containing KLVFF mitigator core and solubilizing residues would improve the interaction between the AAMP and the Aβ full sequence length. The N-methylated peptide, Aβ16−22m previously described to disrupt fibril formation and disassemble preformed fibrils was used as a control peptide because it is similarly designed to block one hydrogen face from β-sheet extension and packing.

Table 1. Modified AAMPs Used to Probe the Assembly and Dissolution of Aβ Fibrils

AAMP	sequence
AAMP-11	RGKLVFFGR
AAMP-12	KGKLVFFGK
AAMP-13	EGKLVFFGE
AAMP-14	(MiniPEG)GKLVFFG(MiniPEG)
AAMP-15	RRRGKLVFFGRRR
AAMP-16	KLVFFGR
AAMP-17	KLVFFG(MiniPEG)
AAMP-18	KLVFFGK
AAMP-19	RGKLVFF
AAMP-20	KLVFFDpgGK
AAMP-21	KGKDibgVFFGK
AAMP-22	KDibgVFFDpgGKKK
AAMP-23	KKKGKLVFFDpgGKKK
AAMP-24	KDibgVFFGKKK
AAMP-25	KLVFFFDpgGKKK
Aβ_{16-22}m	K(Me)LV(Me)FF(Me)AE

Effects of AAMPs on Aβ_{1-40}ThT Fluorescence

Thioflavin T undergoes a characteristic spectral change upon binding to fibrillar species, with maximum emission shifting from 445 to 482 nm (*34*−*36*). The intensity of ThT fluorescence is directly proportional to amyloid fibril formation. However, it has also been shown that fluorescence can result from ThT dye binding to amorphous aggregates though with less intensity (*20*, *37*). Despite this, ThT is useful for following real time formation of amyloid structures and studying the aggregation kinetics. Prior to investigating the effects of AAMPs on Aβ_{1-40} aggregation, the individual peptides were first tested alone to evaluate tendencies to self-aggregate. The individual AAMP solutions were aged in 80 μM PBS (pH 7.4) for 1 week at 37 °C with periodic agitation. Under these conditions, all of the AAMPs exhibited < 10% reduced fluorescence relative to that of

DOI: 10.1021/cn900019r | ACS Chem. Neurosci. (2010), 1, 661–678

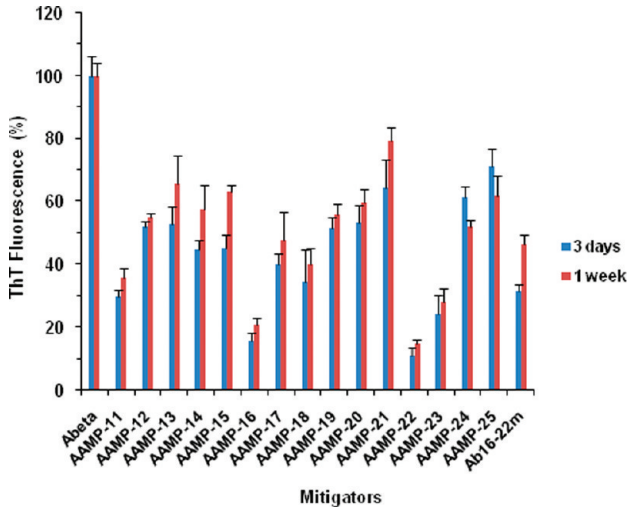

Figure 1. Time dependent ThT fluorescence assay of Aβ/AAMPs. (The final concentration was 40 μM for both $A\beta_{1-40}$ and AAMPs.)

$A\beta_{1-40}$ suggesting minimal formation of thioflavin T active structures.

When $A\beta_{1-40}$ was aged alone, it showed time-dependent increases in fluorescence intensity, indicating aggregation into amyloid fibrils. However, when aged with the various AAMPs at 1:1 molar ratios (40 μM final concentration) with periodic agitation, a reduction of $A\beta_{1-40}$ ThT fluorescence was observed (Figure 1), albeit with different degrees. This suggests a disruption of the $A\beta_{1-40}$ assembly process to form lesser amounts of amyloid or thioflavin T active species. Also, the reduction in fluorescence relative to that of $A\beta_{1-40}$ was influenced greatly by the nature and terminal positioning of the polar residue added.

The AAMPs with N- and C-termini modified using various polar groups showed a reduction in ThT fluorescence between 40 and 70% relative to that of $A\beta_{1-40}$ after 1 week of incubation. In particular, AAMP-11 with polar Arg was the only AAMP with less than 50% reduced fluorescence. The similarity in the percentage of reduced ThT fluorescence indicates that comparable amounts of ThT active structures were formed. When based on ThT alone, one could argue that AAMP-11 is a better disrupter of Aβ fibril formation than the other AAMPs (AAMP-12, AAMP-13, AAMP-14, and AAMP-15) incorporating a polar group on both termini. Also, a concentration dependent experiment was carried out to determine the stoichiometric concentration inhibition mechanism using AAMP-14. We found that AAMP-14 only disrupts at stoichiometric concentrations or molar excess with reduced ThT fluorescence of $>50\%$ relative to that of $A\beta_{1-40}$ alone, in contrast with only 20% reduced fluorescence with substoichiometric ratios (see Supporting Information, Figure S1).

Interestingly, mitigators with polar residues placed on only the C-terminus had an increased reduction in ThT fluorescence (60−80%) as compared to that of the corresponding mitigators with polar groups added to both C- and N-termini (40−70%). For instance, the addition of the Arg residue to only the C-terminus in AAMP-16 was found to exhibit 80% reduced ThT fluorescence. Other AAMPs in the series incorporating MiniPEG (AAMP-17) and Lys (AAMP-18) exhibited a 60% reduction of ThT fluorescence after 1 week of incubation. This suggests a possible effect of terminal polar group position on $A\beta_{1-40}$ fibril formation. However, placing the polar group on the N-terminus, for instance Arg in AAMP-19, showed a reduced fluorescence of 40% as compared to 80% when Arg (AAMP-16) was placed on the C-terminus. This suggests also a difference in the amount or morphology of the amyloid structures formed.

Mitigators incorporating ααAAs and differing numbers of polar residues that were designed to optimize the charge and size of the original mitigator also exhibited reduced fluorescence. The mitigators AAMP-20, AAMP-21, AAMP-24, and AAMP-25 were found to reduce $A\beta_{1-40}$ fluorescence by less than 40%, whereas AAMP-22 and AAMP-23 exhibited 80% reduced ThT fluorescence. On the basis of ThT results, only AAMP-11, AAMP-16, AAMP-22, and AAMP-23 exhibited a higher reduction in ThT fluorescence relative to $A\beta_{1-40}$ than the N-methylated peptide, $A\beta_{16-22}$m previously reported to disrupt fibril formation and to disassemble preformed fibrils (*15*).

As previously described by Austen and co-workers (*31*) AAMP-11 was found to inhibit oligomer formation and prevent $A\beta_{1-40}$ toxicity toward neuroblastoma SH-5Y5Y cells. They reported that an equimolar mixture of $A\beta_{1-40}$/AAMP-11 aged for 12 days under quiescent conditions showed reduced fluorescence of over 80% relative to that of $A\beta_{1-40}$ (*31*). For the same peptide after 7 days aging, however, we report insignificantly lower ThT fluorescence of 63% with periodic sample agitation, as compared to the previously reported result of over 80% reduction under quiescent conditions. Agitation is normally employed to enhance Aβ aggregation enabling analysis on a laboratory time scale, although the fibrils formed are less stable and more toxic (*38*, *39*). Also, a crossover experiment was done with selected AAMPs against an $A\beta_{1-42}$ isoform known to be more toxic and with faster aggregation kinetics than $A\beta_{1-40}$, hence limiting its use in kinetics experiments. The AAMPs tested showed disruptive trends (see Supporting Information, Figure S2) similar to those observed with $A\beta_{1-40}$ suggesting the same mitigator binding site ($A\beta_{1-40}$ central hydrophobic core) as expected and hence identical disruption.

Effect of Various AAMPs on $A\beta_{1-40}$ CD Spectra

The effect of ααAA-AAMPs on $A\beta_{1-40}$ assembly into β-sheet structure was examined using far-UV

DOI: 10.1021/cn900019r | ACS Chem. Neurosci. (2010), 1, 661–678

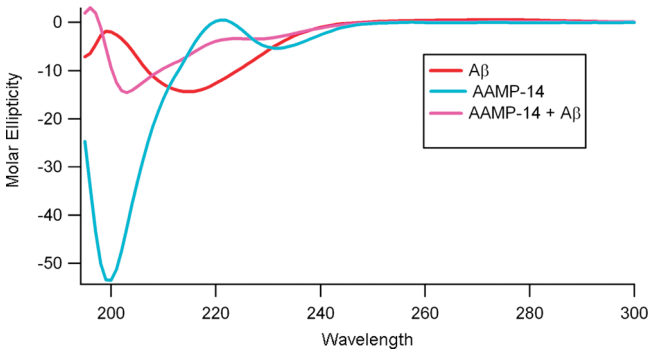

Figure 2. An example of a CD spectra for AAMP-14 alone, Aβ_{1-40} alone, and an Aβ_{1-40}/AAMP-14 equimolar mixture after 1 week of aging. (Final concentration was 40 μM for both Aβ_{1-40} and AAMPs.)

circular dichroism (CD). The CD spectra of monomeric AAMPs and Aβ_{1-40} displayed a strong minimum near 200 nm and maxima near 220 nm, consistent with an unstructured conformation commonly referred to as random coil conformation. After 1 week of aging AAMPs alone at 37 °C while shaking, all exhibited minima in their CD spectra around 200 nm, consistent with unchanged random coil conformation. However, the assembly of Aβ_{1-40} alone after 1 week of incubation exhibited a CD spectra with minima around 217 nm (Figure 2), consistent with aggregation into β-sheet rich assemblies (*25*, *40*). In contrast, when Aβ_{1-40} was aged in the presence of equimolar AAMPs, an unusual CD signature with characteristics of random coil and β sheet was observed, consistent with our previous results for an AAMP-1/Aβ_{1-40} mixture (see Supporting Information, Figure S3 for another example of CD with different AAMPs with identical results.) (*25*). This suggests that our AAMPs delay or disrupt Aβ_{1-40} aggregation into β-sheet rich assemblies.

Effect of AAMPs on Aβ Fibril Morphology

Samples of AAMPs alone, Aβ_{1-40} alone, and mixtures of Aβ_{1-40}/AAMPs, which were prepared for the same time intervals as those of the ThT fluorescence assay, were examined using TEM and AFM. First, samples for the mitigator aged alone were examined to determine the morphology of the aggregates responsible for the observed ThT fluorescence. This is important because Aβ_{1-40} has been shown to aggregate via a nucleation dependent polymerization process (*41*, *42*). Thus, aggregates formed by AAMPs could act as seeds, rapidly increasing the rate of Aβ assembly into fibrils. Peptide mitigators were aged alone in PBS (50 mM at 37 °C with periodic agitation) to investigate their self-aggregation. Topographic images of various samples of AAMPs aged for 1 week displayed sparse distribution of spherical aggregates on the mica surface (see Supporting Information, Figure S4) with mean heights ranging from 2−8 nm.

Effect of AAMPs with Polar Groups Added to Both N- and C-termini on Aβ_{1-40} Fibril Formation

The Aβ_{1-40} sample (40 μM) aged alone showed a dense network of amyloid fibrils averaging 5.4 nm in height and extending several micrometers in length after 3 days of aging (Figure 3A). A predominantly dense network of fibrils averaging 6.9 nm in height and spanning several micrometers in length was observed after 1 week of aging (Figure 3C). The fibrils that formed are consistent with the Aβ_{1-40} aggregation process and fit the proposed hierarchical assembly model (HAM model) (*42*, *43*). The spherical particles observed within a sea of fibrils after 3 days of aging are consistent with results expected with periodic or continuous sample agitation (*44*). The height analysis (Figure 3B and D) shows that mature fibrils with diameter ≥7 nm were predominant after 1 week of aging, which coincides with the results observed with maximum ThT fluorescence.

When Aβ_{1-40} was aged with the equimolar ratio of AAMPs (40 μM) incorporating differently charged polar groups to both C- and N-termini, the normal Aβ_{1-40} aggregation process was disrupted to form either fibrils with different morphologies (appearance and length) or spherical particles. A network of protofibrils and fibrils (Figure 3E) were the major species observed after 3 days of aging Aβ_{1-40} with Arg-containing AAMP-11. The morphology of the AAMP-11 structures (Figure 3G) observed after 1 week of aging for the most part did not change, except that an increase in mean heights was observed as shown by the histogram analysis (Figure 3F and H). Similarly, fibrils/protofibrils (Figure 3I) were observed after 3 days of aging Aβ_{1-40} with equimolar AAMP-12 containing another positively charged group (Lys). After 1 week of incubation of AAMP-12 (Figure 3K), there was increase in both the mean height (Figure 3J and L) and surface coverage of fibrils. Also, when Aβ_{1-40} was aged with AAMP-13 containing a negatively charged Glu residue, protofibrils and fibrils (Figure 3M) were observed after 3 days. Dense networks of beaded fibrils or protofibrils (Figure 3O) were detected after 1 week of incubation with AAMP-13 with height distribution (Figure 3N and P) showing increase in particles size. Interestingly, spherical particles (Figure 3Q) were the major structures observed after 3 days of aging Aβ_{1-40} with AAMP-14 incorporating a neutral MiniPEG group. No fibrillar species (Figure S3, Supporting Information) were observed after 1 week of incubation; only spherical particle clumps were observed resulting in an increase in height as shown by the height histograms (Figure 3R and T). When the number of Arg polar groups was increased to three, as in AAMP-15, fibrils with lengths up to 1−2 μm were observed for a 3 day sample as displayed in AFM

DOI: 10.1021/cn900019r | *ACS Chem. Neurosci.* (2010), *1*, 661–678

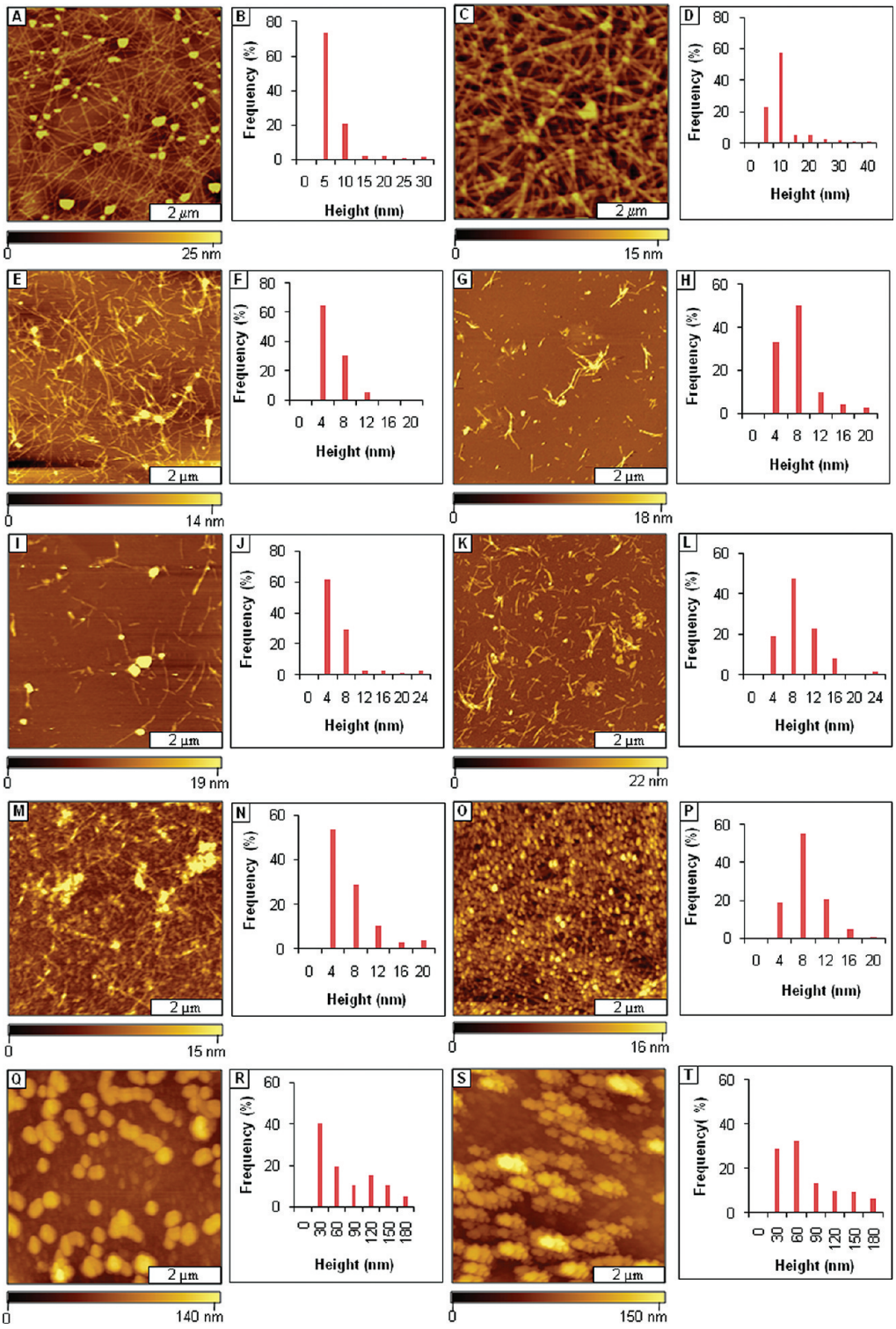

Figure 3. Mitigation of Aβ_{1-40} aggregation by AAMPs with polar groups added to both the C- and N-termini, as viewed by AFM topographs. (A) Fibrils formed after 3 days of incubation by Aβ_{1-40} alone; (B) height analysis for A; (C) fibrils present after 1 week; (D) height analysis for C; (E) fibrils formed after mitigation for 3 days by AAMP-11; (F) height analysis for E; (G) fibrils formed after 1 week; (H) height distribution histogram for G; (I) mixture of spherical and protofibril structures after 3 days of mitigation by AAMP-12; (J) height analysis for I; (K) spherical and short sized fibrils observed after 1 week; (L) height histogram for K; (M) protofibrils present after 3 days with AAMP-13; (N) height analysis for M; (O) fibrils formed after 1 week; (P) height distribution analysis for O; (Q) spherical structures present after mitigation for 3 days by AAMP-14; (R) height distribution for Q; (S) spherical structures observed after 1 week; (T) height analysis for S. (The final concentration was 40 μM for both Aβ_{1-40} and AAMPs.)

DOI: 10.1021/cn900019r | ACS Chem. Neurosci. (2010), 1, 661–678

topographs (Figure 4A). The fibrils observed after 1 week of incubation (Figure 4C) had increased height, as shown by the cursor analysis (Figure 4B and D).

Fibrils were observed to form from aging mixtures of $A\beta_{1-40}$ with AAMP-11 (Figure 3E), which is in disagreement with published results where fibrils were not detected (*31*). The difference in morphology of the particles that formed could be attributed to differences in the aging conditions that were employed. Sample agitation is widely used to expedite amyloid fibril formation. This implies that under quiescent conditions AAMP-11 disrupts fibril formation; however, it only alters $A\beta_{1-40}$ fibril morphology when aggregation rates are increased by agitation. A mixture of short fibrils with lengths spanning few micrometers and linear structures with protofibrillar morphology were observed with AAMP-12 incorporating positively charged Lys. Both AAMP-11 and AAMP-12 alter the $A\beta_{1-40}$ fibrillization pathway forming fibrils that are short in length, more branched, and with lower mean height as compared to those of $A\beta_{1-40}$ fibrils. Surprisingly, this is consistent with SPR studies that showed mitigators (designed also from the KLVFF core) with Lys and Arg polar residues had identical binding affinities for immobilized $A\beta_{10-35}$. However, a dense network of fibrils (Figure 3O) with a beaded morphology was observed when $A\beta_{1-40}$ was aged with AAMP-13 containing negatively charged Glu after 1 week of incubation. The dense network of beaded fibrils observed in AAMP-13 as compared to that in AAMP-12 and AAMP-11 suggests that AAMP-13 is a weaker disrupter of $A\beta_{1-40}$ fibril formation. It is also consistent with findings by Murphy and co-workers from SPR studies that showed lower binding affinity for Aβ10−35 from mitigators with negatively charged polar groups (*30*). The lower binding affinities observed from mitigators with negatively charged polar groups was postulated to be possibly from Coulombic repulsions between the negatively charged polar groups in the mitigator (Glu) and negatively charged residues in Aβ (Glu and Asp) (*12*). In contrast, spherical particles with diameters up to nearly 0.2 μm were observed from aging $A\beta_{1-40}$ in the presence of AAMP-14 (Figure 3Q) with the MiniPEG (neutral) group. The MiniPeg group is a glycol chain and increases the overall hydrophobicity of the peptide. Thus, in this case increased hydrophobicity is more of a factor as compared to Coulombic interaction (AAMP-11 and AAMP-12) because Aβ assembly is initially controlled by hydrophobic interactions. Contrary to results observed for AAMP-14, increasing the overall hydrophilicity of the peptide by the addition of more positively charged Arg for AAMP-15 (three) as compared to AAMP-11 (one) did not necessarily lead to increased disruptive properties, as fibrils were the predominant species observed for both. This suggests the importance of the overall hydrophobicity of the peptide, which has been shown to be involved in the initial process of Aβ assembly.

Effect of AAMPs with Polar Groups Added to the N- or C-Terminus on $A\beta_{1-40}$ Fibril Formation

Surprisingly, AAMPs with polar groups added to only the C-terminus produced particles with a different morphology as compared to those with polar groups added to both termini. For instance, spherical particles (Figure 4E) were the predominant structures observed from aging $A\beta_{1-40}$ with AAMP-16 incorporating Arg on the C-terminus. The height of these particles (Figure 4G) increased up to 100 nm after 1 week of incubation, as shown by height distributions (Figure 4F and H). Mixtures of protofibrils and spherical particles (Figure 4I) were observed after 3 days of aging $A\beta_{1-40}$ in the presence of AAMP-17 containing the neutral MiniPEG group. After 1 week of aging, spherical and linear particles (Figure 4K) with increased heights (Figure 4J and L) were observed. Also, when $A\beta_{1-40}$ was aged with AAMP-18 containing another positively charged group (Lys), spherical particles and protofibrils (Figure 4M) were detected for samples imaged after 3 days. Predominantly, fibrils (Figure 4O) were observed after 1 week of incubation of AAMP-18 exhibiting an increased height distribution as compared to that of spherical/protofibrils observed after 3 days of aging (Figure 4N). When $A\beta_{1-40}$ was aged in the presence of AAMP-19 with polar groups added to the N-terminus, a mixture of spherical and fibrillar structures (Figure 4Q) were observed for samples after 3 days of aging. Predominantly, fibrils spanning a few micrometers (Figure 4S, Supporting Information) and even distribution (Figure 4T) from those of Aβ were observed from samples taken after 1 week of aging.

Modification of only the C-terminal of AAMPs with positively charged groups as in AAMP-16 and AAMP-17 led to the disruption in forming fibrils to produce either nonfibrillar structures or fibrils with different morphologies (fibril length, fibril diameter, and fibril entanglement) as compared to the structure of Aβ alone. Analogues of KLVF with C-terminal modification with Arg or Lys have been shown to have significantly larger binding affinities for Aβ (*30*). Thus, the slight changes observed for the morphology of the particles could be related to the differences in the side chain functionality of the polar groups, where Arg has a more stable positive charge from delocalization as compared to that of Lys. When the positively charged residue is replaced with a neutral group (MiniPEG), similar disruption was observed and could be attributed to enhancing hydrophobic−hydrophobic interactions between Aβ and AAMP-17. Mitigators with their N- or C-terminus modified with the same positively charged polar amino

DOI: 10.1021/cn900019r | *ACS Chem. Neurosci.* (2010), *1*, 661–678

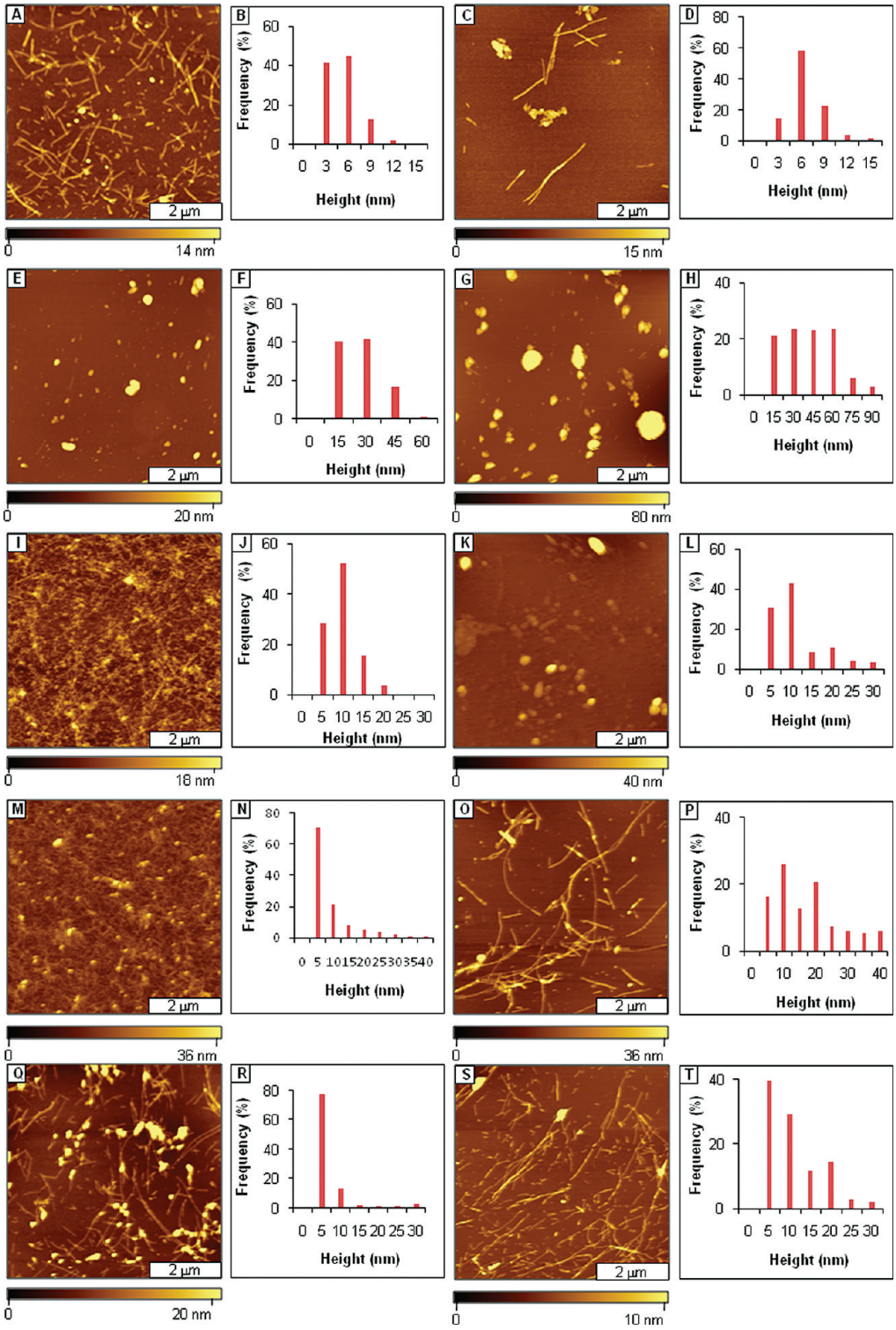

Figure 4. Disruption of Aβ_{1-40} fibril formation by AAMPs with polar groups added to the C- or N-terminus, characterized by tapping mode AFM. (A) Views of short fibrils after 3 days aging Aβ_{1-40} in the presence of AAMP-15; (B) corresponding height distribution for A; (C) after 1 week; (D) height analysis for C; (E) spherical structures detected after 1 week of aging an Aβ_{1-40}/AAMP-16 mixture; (F) corresponding height distribution; (G) after 1 week; (H) height distribution analysis for G; (I) views of spherical and protofibrils formed by an Aβ_{1-40}/AAMP-17 mixture after 3 days of aging; (J) corresponding height analysis; (K) after 1 week; (L) height analysis for K; (M) views of spherical particles and protofibrils formed by Aβ_{1-40} aggregation mitigation by AAMP-18 after 3 days of aging; (N) corresponding height distribution; (O) fibrils detected after 1 week; (P) height analysis for O. (Q) Spherical aggregates and protofibrils observed after 3 days of Aβ_{1-40} mitigation by AAMP-19; (R) height distribution histogram for Q; (S) fibrils were present after 1 week of aging; (T) height analysis for S.

DOI: 10.1021/cn900019r | ACS Chem. Neurosci. (2010), 1, 661–678

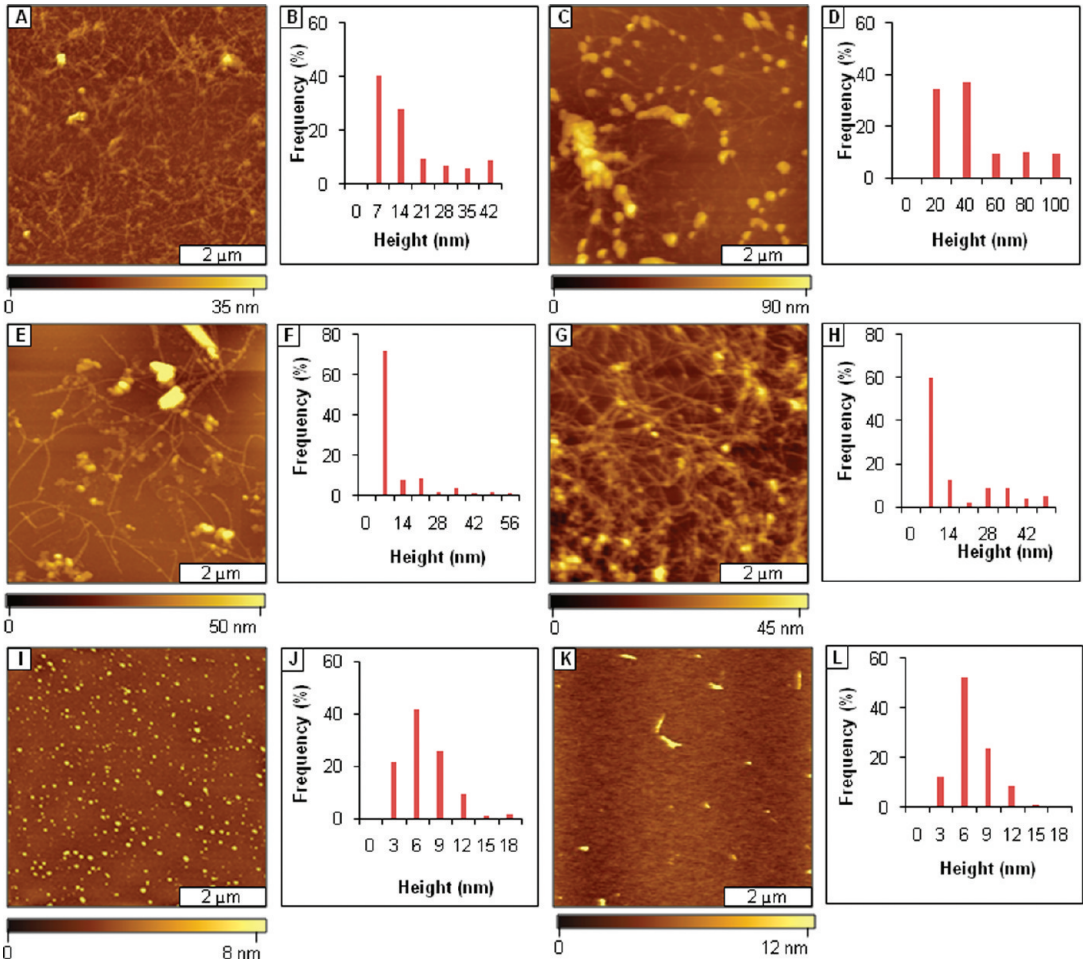

Figure 5. Disruption of $A\beta_{1-40}$ fibril formation by ααAAs-containing AAMPs. (A) Protofibrils and spherical structures observed after 3 days of aging $A\beta_{1-40}$ in the presence of AAMP-20; (B) height distribution for A; (C) spherical structures and fibrils (background) observed after 1 week; (D) corresponding height analysis for C; (E) views of fibrils with some spherical structures detected after 3 days of aging the AB_{1-40}/AAMP-21 mixture; (F) corresponding height distribution; (G) after 1 week; (H) height distribution analysis for G; (I) spherical structures observed for the $A\beta_{1-40}$/AAMP-22 mixture after 3 days of aging; (J) corresponding height analysis; (K) spherical and linear aggregates after 1 week; (L) height analysis for K.

acid residue altered Aβ fibrillization, forming particles with different morphology. For instance, fibrils were predominantly formed in AAMP-19 as compared to spherical particles in AAMP-16 with N- and C-terminal modified with Arg, respectively. This correlates also with binding studies that showed AAMPs with Lys added to the N-terminus had 3-fold lower binding affinities as compared to AAMPs with Lys added to C-terminus.

Effect of ααAA-AAMPs with Polar Groups Added to the C-Terminus on $A\beta_{1-40}$ Fibril Formation

Analogues that incorporate ααAAs were also tested to investigate the effects of varying both ααAAs and polar groups on the morphology of Aβ-AAMP aggregate. Spherical aggregates and isolated protofibrils (Figure 5A) were observed with Dpg-containing AAMP-20 after 3 days of aging. Spherical aggregates (Figure 5C) had grown to ∼100 nm in diameter after 1 week of incubation as discerned from height distribution analysis (Figure 5B and D). Mixtures of spherical aggregates and fibrils/protofibrils (Figure 5E and G) were observed from aging Dibg-containing AAMP-21 after 3 and 7 days of incubation. The height distribution of the particles increased over the same time (Figure 5F and H). When $A\beta_{1-40}$ was aged in the presence of AAMP-22 incorporating two ααAAs, spherical particles (Figure 5I) were observed exclusively after 3 days, while spherical and linear particles (Figure 5K) were observed after 1 week of aging. The diameters and distribution of the particles increased at longer aging times as shown by height analysis (Figure 5J and L). Spherical and linear structures (Figure 6A and C) were observed in AFM topographs of samples after three days and 1 week of incubating $A\beta_{1-40}$ in the presence of AAMP-23, incorporating Dpg and three lysine residues added to both termini.

DOI: 10.1021/cn900019r | ACS Chem. Neurosci. (2010), 1, 661–678

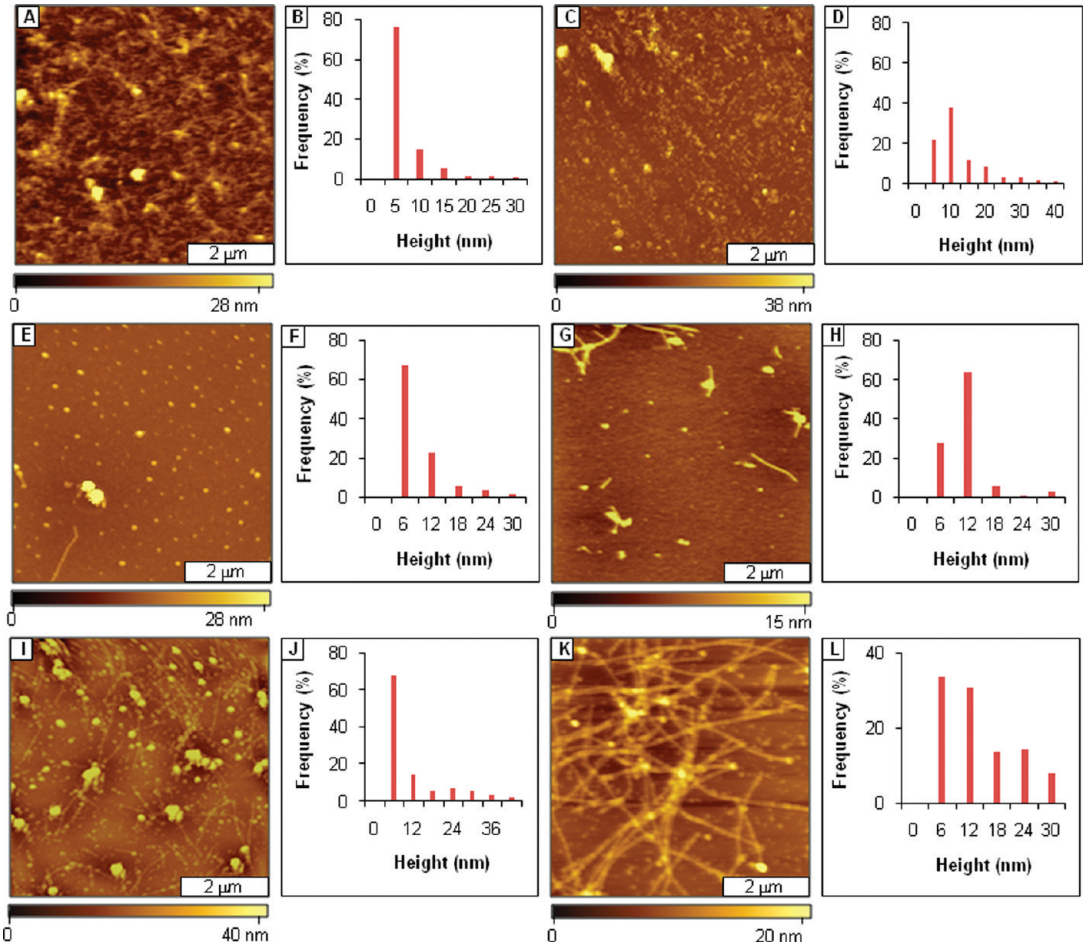

Figure 6. Effects of ααAAs-containing AAMPs on Aβ_{1-40} fibril formation. (A) Protofibrils and spherical structures were observed after 3 days of aging Aβ_{1-40} in the presence of AAMP-23; (B) height distribution for A; (C) spherical structures and linear structures observed after 1 week; (D) corresponding height analysis; (E) spherical structures observed after 1 week of aging the Aβ_{1-40}/AAMP-24 mixture; (F) height distribution analysis for E; (G) rod-like fibrils and spherical aggregates observed after 1 week; (H) corresponding histogram analysis; (I) spherical and protofibrillar structures observed after aging Aβ_{1-40}/AAMP-25 for 3 days; (J) corresponding height analysis; (K) after 1 week (L); height analysis for K.

AAMP-20 and AAMP-21 are similar in design with AAMP-18 and AAMP-12 except for ααAA incorporated in their core. Mixtures of spherical aggregates and fibrils were observed with both AAMP-20 and AAMP-21 with diameters of spherical aggregates spanning up to 0.1 μm as compared to those of primarily fibrils for AAMP-18 and AAMP-12, although with different morphologies as compared to those of Aβ_{1-40}. When the number of Lys were increased to three and another ααAAs introduced as in AAMP-22, compared to AAMP-20 with only one Lys and ααAA, no fibrillar structures were observed. This is also consistent with the 80% reduced fluorescence observed relative to that of Aβ_{1-40}. Also, increasing the length of polar residues on each termini to three, as in AAMP-23, resulted in the disruption of fibrils as compared to AAMP-20 (with one polar group and similar ααAAs) and AAMP-15 (with no ααAAs but same number of polar groups), both showing fibrils as major species after 1 week of incubation. This suggests synergistic contributions from both ααAAs as well as polar groups on the disruption of Aβ_{1-40} fibril formation. This is consistent with the increased solubility of Aβ/AAMP aggregate and steric factors, crucial in our mitigator design.

Spherical structures (Figure 6E) were observed after 3 days of aging a mixture of Aβ_{1-40} and AAMP-24. After 1 week of incubation, spherical aggregates and protofibrils or linear structures (Figure 6G) were the predominant structures. However, after 3 days of incubation of an Aβ_{1-40}/AAMP-25 mixture, spherical aggregates and protofibrils (Figure 6I) were observed. After 1 week of aging, fibrils (Figure 6K) were more abundant. For all the AAMPs, particles that formed were observed to increase in height after longer aging, as shown by height distributions (Figure 6B, D, F, H, J, and L).

The different morphologies of the particles observed with AAMP-24 as compared to those in AAMP-25 can be attributed to the steric difference between the

DOI: 10.1021/cn900019r | ACS Chem. Neurosci. (2010), 1, 661–678

αααAAs. Mixtures of spherical particles and protofibrils were formed with AAMP-24, which contains more sterically hindered Dibg (isobutyl side chains) as compared to the fibrils in AAMP-25, which incorporate Dpg (*n*-propyl side chains). This highlights the important role of steric hindrance in the mechanisms (blocking face of aggregation) for disruption of Aβ fibrillization. Also, the morphologies of resultant assemblies were confirmed with TEM (see Supporting Information, Figure S5).

Disassembly of Preformed Fibrils

It has been shown that the presence of fibrils in the brain nucleates further deposition of plaques in AD (*45*). It was previously stated that a dynamic equilibrium exists between monomers/dimers and fibrils (*22*, *46*, *47*). This makes agents that induce fibril disassembly an attractive source for the development of new therapeutics that will reduce or eliminate plaques in the brain. Previously, β-sheet breaker (*22*) and N-methylated peptides (*15*, *46*) have been shown to also disassemble preformed fibrils. Herein, we evaluate also whether the designed AAMPs disassemble Aβ preformed fibrils. Mature fibrils were formed by incubating Aβ_{1-40} for 1 week at 37 °C in PBS (pH 7.4) while agitating. Equimolar mixtures of Aβ_{1-40} preformed fibrils and AAMPs were aged for 24 h to evaluate their potential for disassembly. The extent to which AAMPs induced fibril disassembly was monitored using ThT fluorescence, as well as with images acquired with AFM and TEM. Results of ThT fluorescence are shown in Figure 7 as the percentage relative to that of Aβ_{1-40}.

Various AAMPs exhibit reduced fluorescence of more than 50% relative to that of Aβ_{1-40}. The N-methylated control peptide Aβ16−22m, which has been shown to disassemble fibrils, displayed 40% reduced fluorescence (*15*). On the basis of ThT fluorescence only, various AAMPs tested exhibited reduced fluorescence comparable to that of the N-methylated control peptide. After 24 h, there is no significant difference in ThT fluorescence observed for AAMPs incorporating polar groups on the N-and C-termini (AAMP-11−15), C-terminus (AAMP-16−18), N-terminus (AAMP-19), or αααAA-containing AAMPs (AAMP-20−25). It should also be noted that the reduced fluorescence exhibited by the various AAMPs do not necessarily indicate the absence of fibrils. This is because inhibitor or disrupter molecules can bind to fibrils displacing the bound ThT molecule resulting in reduced fluorescence.

Size and Morphology of Structures Formed by the Disassembly of Preformed Fibrils by Various AAMPs

Parallel AFM experiments were conducted for samples prepared at the same time as those for ThT fluorescence.

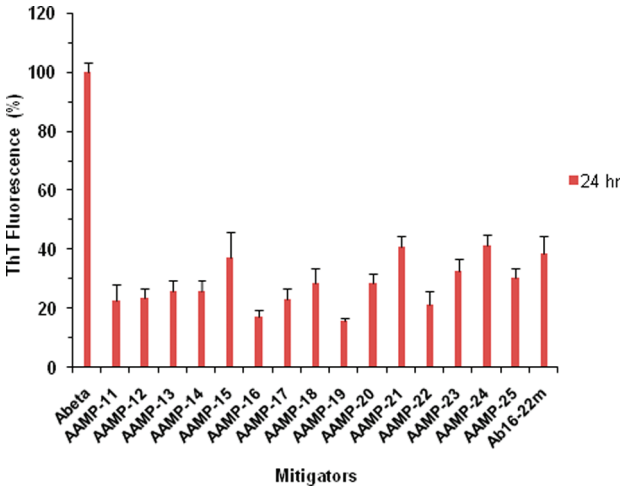

Figure 7. Fibril disassembly by various AAMPs as monitored by ThT fluorescence, presented as the percent relative to that of Aβ_{1-40}.

A dense network of fibrils with a mean height of 7.9 nm was observed from a topographic AFM image of Aβ_{1-40} sample after 1 week of aging (Figure 8A). Similar observations were found with TEM micrographs, which displayed fibrils spanning several micrometers in length (data not shown). Fibrils and protofibrils were the major structures observed with the disassembly of preformed fibrils by AAMP-11 (Figure 8C), AAMP-12 (Figure 8E), and AAMP-15 (Figure 8K), which all have polar groups added to both the C- and N-termini. Spherical aggregates were the main structures observed after the disassembly of preformed fibrils by AAMP-13 (Figure 8G) and AAMP-14 (Figure 8I), which incorporate Glu and PEG chains, respectively, into the C- and N-termini. Predominantly, intact fibrils and isolated spherical particles were the major products observed for the disassembly of preformed fibrils by AAMP-16 (Figure 8M), AAMP-17 (Figure 8O), and AAMP-18 (Figure 8Q) with different polar groups added only to the C-terminus. Partially disassembled fibrils were observed for AAMP-19 (Figure 8S) with polar groups added to only the N-terminus. Figure 8B, D, F, H, J, L, N, P, R, and T shows the corresponding height distributions from an analysis of multiple cursor profiles.

Fibrillar structures were the predominant structures formed from the disassembly by AAMP-11, AAMP-12, AAMP-15, AAMP-16, AAMP-17, AAMP-18, and AAMP-19. However, the surface coverage and morphology (distribution, appearance, length, etc.) of the fibrillar structures formed indicates partial disassembly. For instance, fibrillar structures observed from Aβ_{1-40} fibril disassembly by AAMP-15, AAMP-17, and AAMP-18 showed nucleation units along the fibril length. This is an indication of immature fibrils or protofibrillar structures, which are precursors of mature fibril formation.

DOI: 10.1021/cn900019r | *ACS Chem. Neurosci.* (2010), *1*, 661–678

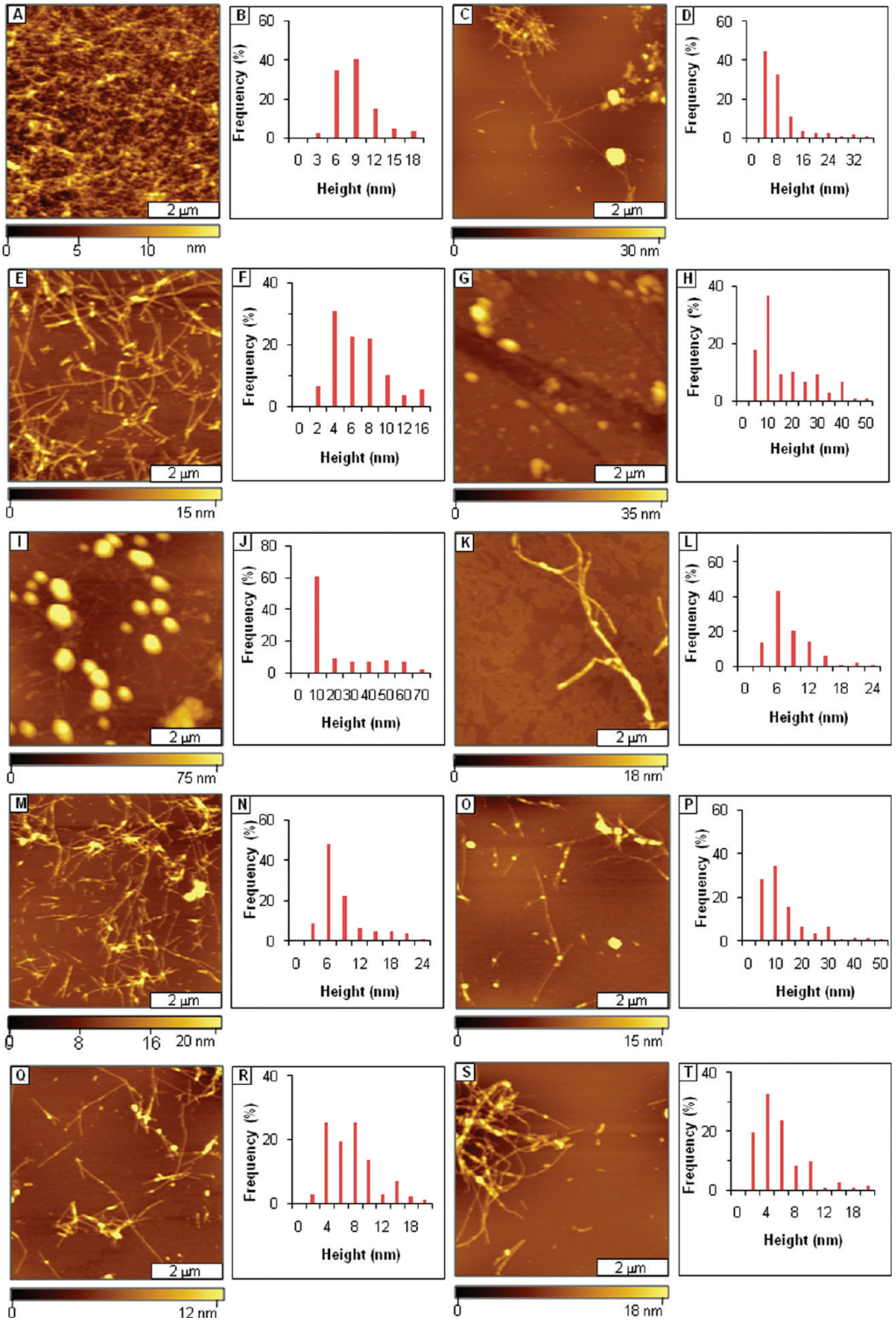

Figure 8. Disassembly of preformed fibrils of Aβ_{1-40}. (A) Control sample of Aβ_{1-40} fibrils. (B) Corresponding height histogram. (C) Fibrils and spherical structures after disassembly by AAMP-11. (D) Histogram analysis for C. (E) Partial disassembly by AAMP-12. (F) Height histogram analysis for E. (G) Spherical particles formed by AAMP-13 fibril disassembly. (H) Height analysis for G. (I) Spherical aggregates and fibrils (background) formed from disassembly by AAMP-14. (J) Corresponding height analysis. (K) Isolated fibrils present from disassembly by AAMP-15. (L) Height histogram for K. (M) Mixture of short and long fibrils observed from disassembly by AAMP-16. (N) Corresponding height analysis. (O) Fibrils showing beaded sections for Aβ_{1-40} fibril disassembly by AAMP-17. (P) Corresponding height histogram. (Q) Fibrils showing nucleation units for mature fibrils after disassembly by AAMP-18. (R) Corresponding height analysis. (S) Partial preformed fibril disassembly observed with AAMP-19. (T) Height histogram for O.

DOI: 10.1021/cn900019r | ACS Chem. Neurosci. (2010), 1, 661–678

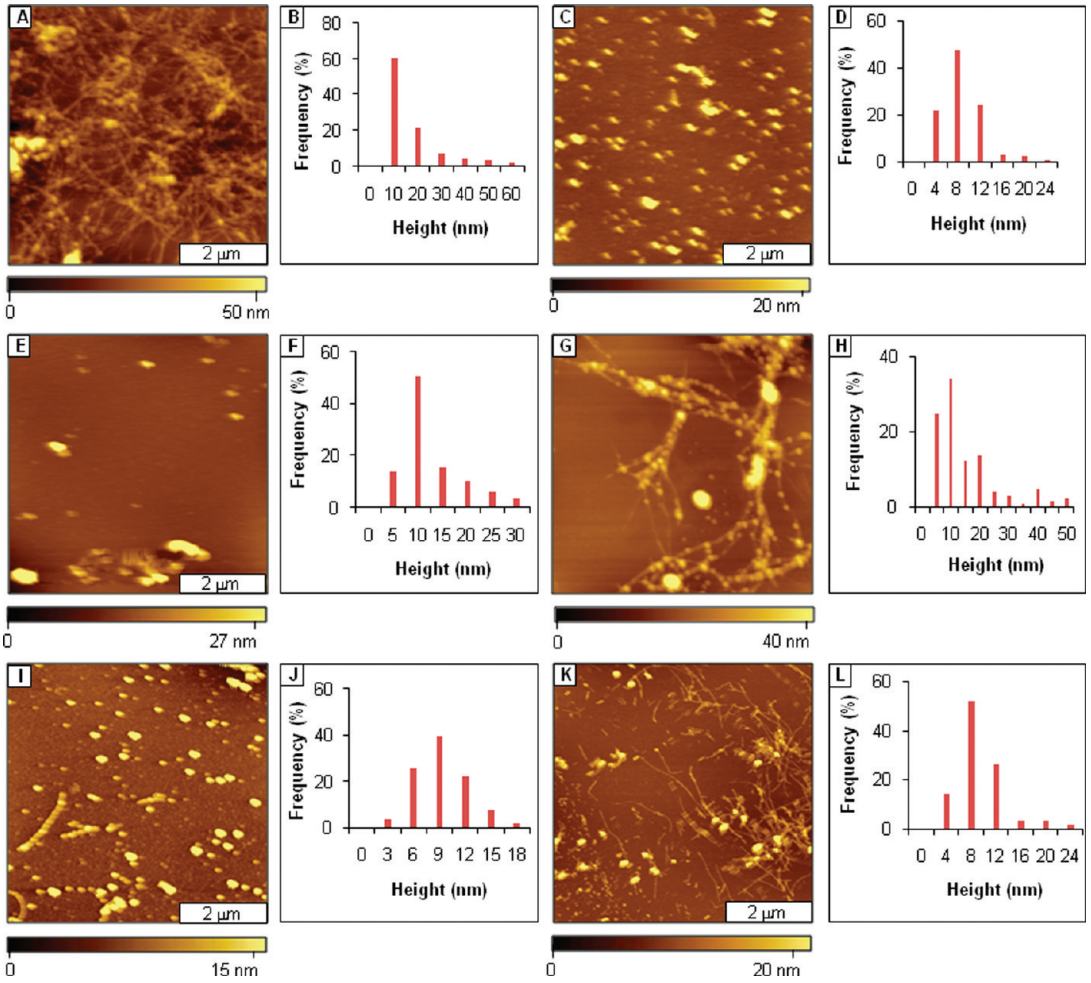

Figure 9. Disassembly of Aβ_{1-40} preformed fibrils imaged using tapping mode AFM. (A) Fibril disassembly by AAMP-20. (B) Corresponding height histogram. (C) Spherical structures were observed with disassembly by AAMP-21. (D) Height analysis for C. (E) Spherical structures with disassembly by AAMP-22. (F) Corresponding height histogram. (G) Fibrils with beaded morphology observed from disassembly by AAMP-23. (H) Height analysis for G. (I) Spherical aggregates and isolated protofibrils formed from disassembly by AAMP-24. (J) Height analysis for I. (K) Fibrils and some spherical species observed from fibril disassembly by AAMP-25. (L) Corresponding height analysis. (The final concentration was 40 μM for both Aβ_{1-40} and AAMPs.)

In addition, there is evidence of fibril breakage as shown by the presence of fibrils with lengths less than a micrometer (AAMP-16) as compared to those of preformed Aβ_{1-40} fibrils which span several micrometers. The only exceptions are AAMP-13 and AAMP-14 where spherical particles with diameters up to 0.1 μm were formed. Interestingly, these two mitigators incorporate oligolysine and PEG chains, respectively, on both termini. This underscores the contributions of terminal chains either hydrophobic or hydrophilic in the mechanism of disassembly for preformed fibrils.

When ααAA-containing AAMPs were mixed with preformed fibrils, fibrils/protofibrils (Figure 9A and K) were the major species with disassembly by Dpg-containing AAMP-20 and AAMP25 as compared to mainly spherical particles (Figure 9C and I) observed with Dibg containing AAMP-21 and AAMP-24. Interestingly, spherical particles (Figure 9E) with a mean height of 11.2 nm were the major structures of disassembly when both ααAAs (Dpg and Dibg) were incorporated in a mitigator as in AAMP-22. Also, extending the oligolysine chain on both termini as in Dpg-containing AAMP-23 (Figure 9G) evidenced no fibrils in AFM images, suggesting that the oligolysine chain plays a role in the disassembly of preformed fibrils. Figure 9B, D, F, H, J, and L provides corresponding analysis of the height distribution of particles from AFM cursor measurements.

The steric nature of ααAAs has a role in the disassembly process as evidenced from spherical particles formed by the diisobutyl side chain containing AAMP-21 and AAMP-24, as compared to fibrillar structures formed with a dipropyl side chain containing AAMP-20 and AAMP-25. The distribution of ααAAs in the KLVFF motif is a factor in the disassembly of preformed fibrils. For instance, fibrillar structures were the major species formed by AAMPs incorporating ααAAs

DOI: 10.1021/cn900019r | ACS Chem. Neurosci. (2010), 1, 661–678

Table 2. Summary of Results from the Assembly and Disassembly of A$\beta_{1\text{-}40}$ in the Presence of Various Mitigators

	assembly				disassembly	
	3 days		1 week		24 h	
AAMPs	aggregate type	mean height (nm)	aggregate type	mean height (nm)	aggregate type	mean height
Aβ_{1-40}	fibrils	5 ± 2	fibrils	7 ± 4	fibrils	8 ± 3
AAMP-11	protofibrils/fibrils	4 ± 2	protofibrils/fibrils	7 ± 3	spherical/protofibrils	7 ± 4
AAMP-12	protofibrils/spherical	5 ± 3	rod shaped fibrils	8 ± 3	spherical/fibrils	6 ± 3
AAMP-13	protofibrils/fibrils	6 ± 3	protofibrils/beaded fibrils	7.2 ± 2	spherical	16 ± 11
AAMP-14	spherical	28 ± 13	spherical	40 ± 21	protofibrils/spherical	20 ± 11
AAMP-15	protofibril/linear	4 ± 2	protofibril/rod like fibrils	6 ± 2	spherical	7 ± 4
AAMP-16	spherical	21 ± 10	spherical	36 ± 15	fibrils/spherical	8 ± 5
AAMP-17	spherical	8 ± 4	spherical	10 ± 4	spherical/protofibrils	7 ± 4
AAMP-18	protofibrils/spherical	6 ± 3	fibrils	8 ± 3	protofibrils/fibrils	12 ± 7
AAMP-19	spherical/protofibrils	6 ± 3	linear/fibrils	10 ± 4	fibrils	5 ± 4
AAMP-20	protofibrils	7 ± 3	spherical/linear	24 ± 12	protofibrils/fibrils	10 ± 5
AAMP-21	protofibrils	5 ± 3	fibrils	8 ± 5	spherical/protofibrils	7 ± 4
AAMP-22	spherical	6 ± 2	spherical	6 ± 3	spherical/linear	11 ± 7
AAMP-23	spherical/linear	5 ± 2	linear/spherical	10 ± 5	spherical	13 ± 8
AAMP-24	spherical	9 ± 4	spherical, linear	6 ± 2	spherical/protofibrils	8 ± 3
AAMP-25	spherical, protofibrils	6 ± 3	fibrils	12 ± 7	fibrils	8 ± 4
Aβ_{16-22}	spherical	11 ± 5	spherical/fibrils	16 ± 10	spherical	36 ± 20

outside the KLVFF region (AAMP-20 and AAMP-25) as compared to the spherical structures observed with ααAAs placed in the KLVFF core, which is consistent with our previous observation (*27*). Also, increasing the hydrophobicity or steric nature of the mitigator by incorporating two ααAA as in AAMP-22 induces disassembly of preformed fibrils to form spherical particles exclusively. Although not conclusive, greater surface coverage of disassembled fibrils was observed with AAMP-20 than in the case of AAMP-25 with one and three C-terminal lysines, respectively. This suggests that the length of the lysine chain plays a role in the disassembly process. The same trend of the lysine chain length effect is also seen with AAMP-23 with three lysines added to both termini, where no fibrils were detected as expected suggesting that the added chain also contributes to the disassembly of preformed fibrils. This shows that the disassembly of preformed fibrils is a synergistic combination of the influences of ααAAs as well the length of the polar groups.

A comparison of results for the various AAMPs from analyses of the AFM images observed for the assembly and disassembly of the various mitigators are summarized in Table 2. Our studies demonstrate that terminal modifications of the mitigator core sequence (KLVFF) with different polar groups altered Aβ fibrillization yielding particles with different morphologies and sizes. Different results were obtained with modification of only the C-terminus as compared to changes for both N- and C- termini. For instance, mitigator AAMP-16 with the C-terminal modified with Arg was found to be a potent disrupter of Aβ_{1-40} fibril assembly, forming spherical aggregates. This is consistent with the previously reported use of Arg to solubilize inhibitors of Aβ_{1-42} (*48*) and α-synuclein (*49*) fibrillogenesis, and protect differentiated SHSY-5Y neuroblastoma cells against Aβ toxicity. Also, as a result of terminal modifications with different polar groups, potent mitigators of Aβ_{1-40} fibrillization were found where the most interesting are the ones with neutral MiniPEG polar groups. This is because previous designs mostly used positively charged amino acids such as Lys or Arg which makes peptide delivery through the brain barrier difficult, leading to accumulation and toxicity as previously observed at high doses with our original mitigator with six Lys residues (*32*). Thus, this study serves as a foundation for the future design of more effective peptides with increased systemic bioavailability and for optimal use in vivo.

Smaller-sized spherical particles were observed for disruption by AAMP-17 as compared to AAMP-14, with the C-terminus or the C- and N-termini modified with MiniPEG, respectively. This indicates that the N-terminal modification enhances aggregation to form larger assemblies. We have previously reported similar results where large sizes of particles formed with N-terminal modification of ααAA-KLVFF compared to C-terminal modification using six oligolysine chains (*25*). The particle size difference is closely

DOI: 10.1021/cn900019r | *ACS Chem. Neurosci.* (2010), *1*, 661–678

associated with the disruption of the hydrophobic C-terminal group (*50*), which has more impact on aggregation than the hydrophilic N-terminal (*51*).

The different morphologies of particles formed with AAMP-19 (fibrils) and AAMP-16 (spherical aggregates) are attributable of the N- and C-terminal modifications, respectively. Through SPR binding studies, Murphy and co-workers have shown that AAMPs with positively charged polar groups placed on the N-terminus have a 3-fold lower affinity for immobilized $A\beta_{10-35}$ than the ones placed on the C-terminus (*30*). From SPR and our AFM studies, it can be concluded that mitigators with a higher affinity for the target $A\beta_{1-40}$ are better disrupters of Aβ fibrillization.

The AAMPs incorporating ααAAs were better disrupters of Aβ fibrillization as compared to AAMPs without ααAAs. For instance, linear structures and fibrils were formed from the incubation of $A\beta_{1-40}$ in the presence of ααAA-containing AAMP-20 and AAMP-18, respectively. This is because incorporating ααAAs in the AAMP core forces the peptide to adopt an extended conformation that is ideal for interacting with $A\beta_{1-40}$ through side chain−side chain hydrophobic interactions. Also, incorporation of ααAAs into the mitigator core increases its hydrophobic character and, in essence, impacts $A\beta_{1-40}$ assembly since the initial aggregation is controlled by hydrophobic interactions. Mitigator AAMP-22 incorporating two ααAAs in the KLVFF motif and containing three lysines on the C-terminus was found to have similar disruptive properties as compared to our previously reported AAMP-3 (*27*) with six lysines (*25*). This shows that the number of lysines can be reduced without affecting the solubility and disruptive properties of the mitigator.

Mitigators incorporating ααAAs that disrupted fibril formation also disassembled preformed fibrils, which underscore the importance of steric used in the design of these mitigators. This was compared to the primary fibrils/protofibrils observed in AAMPs without ααAAs as with AFM and TEM data. Mitigators that disassembled preformed fibrils to produce prefibrillar assemblies suggest that equilibrium exists between fibrils and prefibrillar aggregates. Topographic AFM data of the disassembly of preformed fibrils show agreement with data from ThT fluorescence. The lower percent ThT fluorescence exhibited by AAMP/$A\beta_{1-40}$ mixtures is consistent with the observations of lower surface coverage of fibrils. Peptides, which have their termini modified with Lys, Arg, Glu, and glycol chains have been shown to be effective at disrupting fibril formation as well as protecting against neuronal toxicity (*15*, *18*, *19*, *31*). Mitigators, AAMP-21, AAMP-22, and AAMP-23 induced the disassembly of preformed fibrils to a degree similar to that of N-methylated peptide, Aβ16−22m, which was previously shown to disassemble preformed fibrils (*15*). The N-methylated Aβ16−22m disassembled preformed fibrils and yielded large spherical aggregates with mean heights of 35.6 nm. In contrast, smaller aggregates were observed with ααAA-AAMPs. The difference in the height of assemblies that formed can only be attributable to the added polar groups. Thus, polar groups play a role in determining the size of assemblies formed. We hypothesize that substitution of the hydrogen atom on the α-carbon of certain amino acids in the critical KLVFF region with an alkyl substituent yields a more hydrophobic peptide. Initial assembly of Aβ oligomers is controlled by the hydrophobic side chains. Thus, increasing the hydrophobicity of this region should also enhance interactions between Aβ and the mitigator, leading to both the disruption of Aβ assembly into fibrils as well as the disassembly of preformed fibrils. The mechanism of disassembly is believed to occur by mitigator monomers binding to the end of fibrils and shifting equilibrium toward prefibrillar assemblies. Thus, this study can guide future designs of dissolution agents.

In addition, there is increasing evidence that equilibrium exists between fibrils and monomers (*47*, *52*, *53*). Mitigator $KLVFFK_6$ was previously shown by Murphy and co-workers to alter the $A\beta_{1-40}$ fibrillization process, forming fibrils with different morphologies that were protective against Aβ cytotoxicity. The nontoxic nature of these fibrils is believed to be because they are stable to the equilibrium change unlike Aβ fibrils which are in constant equilibrium with the more toxic oligomeric assemblies (*13*). Thus, future cytotoxicity experiments on our mitigators that form fibrils with morphologies different from those of $A\beta_{1-40}$ fibrils will further provide a basis for the design of mitigators that may result in fibrils that are stable and protect against neurotoxicity.

Methods

Peptide Synthesis

The various AAMPs were synthesized from 9*H*-fluoren-9-ylmethoxycarbonyl (Fmoc) amino acids using solid phase peptide synthesis on PAL-PEG-PS resin or Rink amide ChemMatrix resin. Coupling of individual amino acids was achieved using previously described methods (*54*−*56*). After the last amino acid was coupled, the peptides were deprotected and cleaved from the resin by treatment with cleavage cocktail [88% trifluoroacetic acid (TFA), 5% H_2O, 5% phenol, and 2% TIPS]. The peptides were precipitated from the cocktail solution with cold diethyl ether and then dissolved in water/acetonitrile, and lyophilized. The crude peptides were purified by reversed phase HPLC using a 10% to 70% B linear gradient over 60 min [Waters C_4 100 Å column using solvent A (water and 0.1% TFA) and solvent B (acetonitrile and 0.1% TFA)]. The purity of the peptides was checked by analytical HPLC and the masses confirmed by ESI-MS. The percent peptide content was verified by amino acid analysis.

DOI: 10.1021/cn900019r | *ACS Chem. Neurosci.* (2010), *1*, 661–678

Peptide Monomerization

Lyophilized Aβ_{1-40} purchased from Invitrogen Corporation (Carlsbad, CA, USA) was pretreated to form monomeric solutions following our previously published protocol (*57*). Briefly, Aβ_{1-40} was dissolved in neat TFA at 1 mg/mL, sonicated for 10−20 min, and removed using a centrivac, yielding a dark yellow oil. The dark oil was dissolved in 1 mL of hexafluoroisopropanol (HFIP) at 1 mg/mL and aged at 37 °C for 1 h, after which HFIP was removed, yielding a white powder. The white powder was redissolved in HFIP and split into 0.25 mg fractions based on the assumption that at this point in the preparation the mass of Aβ_{1-40} was 50%. The 0.25 mg fractions were aged for 1 h upon which HFIP was removed, and the white powder product was lyophilized overnight. The lyophilized white powder was dissolved in 2 mM NaOH and PBS (100 mM and 300 mM NaCl, pH 7.4) at 1:1 and centrifuged for 20 min at 13,000*g*, which was then ready for the aggregation assay. The supernatant was subjected to amino acid analysis to determine the net peptide content.

Thioflavin T (ThT) Fluorescence Aggregation Assays

Monomerized Aβ_{1-40} was incubated alone and with the various AAMPs at 37 °C while shaking in PBS buffer (50 mM and 150 mM NaCl, pH 7.4). At different stages of aggregation, 10 μL of sample, 10 μL of 100-μM ThT stock solution in water, and 180 μL of PBS were mixed in a low binding 96 well plate with a clear bottom (Corning or Falcon). ThT fluorescence was measured using a BMG, LAB TECH spectrophotometer (excitation at 440 nm and emission at 480 nm).

Circular Dichroism

Samples of monomerized Aβ_{1-40} alone and in the presence of various AAMPs were incubated at 37 °C for 1 week while shaking. The CD spectra were recorded at room temperature using an Aviv CD spectrometer from 190 to 300 nm. The wavelength step was 1 nm, 3 scans were taken, and the averaging time was 1 s at each wavelength.

Atomic Force Microscopy

A 10 μL sample aliquot (diluted 2-fold) was adsorbed onto a freshly cleaved mica(0001) (Ruby muscovite mica, S&J Trading Co., NY) surface for 5−10 min. Excess liquid was removed by absorption onto a filter paper or lab tissue. Salts and excess unbound peptide were washed gently from the surface using 40 μL (3×) deionized water. Tapping mode images were acquired with a model 5500 atomic force microscope (AFM) equipped with PicoScan v5.3.3 software (Agilent Technologies AFM, Inc. Chandler, AZ). Cantilevers (NSL-20) from Nanoworld Holdings AG (Schaffhausen, Switzerland) were used for imaging samples in air. The cantilever was driven to oscillate at 175 ± 10 kHz for ambient AFM characterizations.

Transmission Electron Microscopy

The formation of fibrils was verified by TEM analysis of negatively stained samples. Samples from aged solutions were placed as a droplet on a carbon-coated copper grid (EMS 400-CU) for 1−2 min. The excess sample was wicked away using a filter paper. The sample was washed by placing the grid onto a droplet of water and then stained using 2% uranyl acetate. Images were recorded using a JEOL 100 CX TEM, 80 kV accelerating voltage.

Supporting Information Available

Concentration dependent study of the assembly of Aβ_{1-40} in the presence of AAMP-14; assembly of Aβ_{1-42} in the presence of ααAA-AAMPs; example CD signatures obtained for Aβ_{1-40} mitigation; spherical aggregates observed after one week of aging the various AAMPs alone; morphologies of various surface structures observed after one week of aging Aβ_{1-40} in the presence of various AAMPs with and without ααAAs. This material is available free of charge via the Internet at http://pubs.acs.org.

Author Information

Corresponding Author

* Corresponding author. Department of Chemistry, Louisiana State University, 232 Choppin Hall, Baton Rouge, LA 70803. Phone: 225-578-8942. E-mail: jgarno@lsu.edu.

References

1. Selkoe, D. J. (1991) The molecular pathology of Alzheimers-disease. *Neuron 6*, 487–498.

2. Selkoe, D. J. (2003) Folding proteins in fatal ways. *Nature 426*, 900–904.

3. Tycko, R. (2003) Insights into the amyloid folding problem from solid-state NMR. *Biochemistry 42*, 3151–3159.

4. Baglioni, S., Casamenti, F., Bucciantini, M., Luheshi, L. M., Taddei, N., Chiti, F., Dobson, C. M., and Stefani, M. (2006) Prefibrillar amyloid aggregates could be generic toxins in higher organisms. *J. Neurosci. 26*, 8160–8167.

5. Chromy, B. A., Nowak, R. J., Lambert, M. P., Viola, K. L., Chang, L., Velasco, P. T., Jones, B. W., Fernandez, S. J., Lacor, P. N., Horowitz, P., Finch, C. E., Krafft, G. A., and Klein, W. L. (2003) Self-assembly of A beta(1−42) into globular neurotoxins. *Biochemistry 42*, 12749–12760.

6. Hardy, J., and Selkoe, D. J. (2002) Medicine - The amyloid hypothesis of Alzheimer's disease: Progress and problems on the road to therapeutics. *Science 297*, 353–356.

7. Walsh, D. M., and Selkoe, D. J. (2004) Oligomers in the brain: The emerging role of soluble protein aggregates in neurodegeneration. *Protein Peptide Lett. 11*, 213–228.

8. Walsh, D. M., and Selkoe, D. J. (2007) A beta Oligomers - a decade of discovery. *J. Neurochem. 101*, 1172–1184.

9. Fukumoto, H., Tokuda, T., Kasai, T., Ishigami, N., Hidaka, H., Kondo, M., Allsop, D., and Nakagawa, M. (2010) High-molecular-weight {beta}-amyloid oligomers are elevated in cerebrospinal fluid of Alzheimer patients. *FASEB J. 24*, 2716–2726.

10. Kemsley, J. (2009) Analyzing protein Drugs. *Chem. Eng. News*20–23.

11. Tjernberg, L. O., Lilliehook, C., Callaway, D. J. E., Naslund, J., Hahne, S., Thyberg, J., Terenius, L., and Nordstedt, C. (1997) Controlling amyloid beta-peptide fibril formation with protease-stable ligands. *J. Biol. Chem. 272*, 12601–12605.

12. Tjernberg, L. O., Naslund, J., Lindqvist, F., Johansson, J., Karlstrom, A. R., Thyberg, J., Terenius, L., and Nordstedt, C.

DOI: 10.1021/cn900019r | *ACS Chem. Neurosci.* (2010), *1*, 661–678

(1996) Arrest of beta-amyloid fibril formation by a pentapeptide ligand. *J. Biol. Chem. 271*, 8545–8548.

13. Ghanta, J., Shen, C.-L., Kiessling, L. L., and Murphy, R. M. (1996) A strategy for designing inhibitors of b-amyloid toxicity. *J. Biol. Chem. 271*, 29525–29528.

14. Etienne, M. A., Aucoin, J. P., Fu, Y., McCarley, R. L., and Hammer, R. P. (2006) Stoichiometric inhibition of amyloid beta-protein aggregation with peptides containing alternating alpha, alpha-disubstituted amino acids. *J. Am. Chem. Soc. 128*, 3522–3523.

15. Gordon, D. J., Sciarretta, K. L., and Meredith, S. C. (2001) Inhibition of β-amyloid(40) fibrillogenesis and disassembly of β-amyloid(40) fibrils by short β-amyloid congeners containing N-methyl amino acids at alternate residues. *Biochemistry 40*, 8237–8245.

16. Sciarretta, K. L., Gordon, D. J., and Meredith, S. C. (2006) Peptide-based inhibitors of amyloid assembly. *Methods Enzymol. 413*, 273–312.

17. Pallitto, M. M., Ghanta, J., Heinzelman, P., Kiessling, L. L., and Murphy, R. M. (1999) Recognition sequence design for peptidyl modulators of beta-amyloid aggregation and toxicity. *Biochemistry 38*, 3570–3578.

18. Gordon, D. J., Tappe, R., and Meredith, S. C. (2002) Design and characterization of a membrane permeable N-methyl amino acid-containing peptide that inhibits Aβ1−40 fibrillogenesis. *J. Pept. Res. 60*, 37–55.

19. Gordon, D. J., and Meredith, S. C. (2003) Probing the role of backbone hydrogen bonding in beta-amyloid fibrils with inhibitor peptides containing ester bonds at alternate positions. *Biochemistry 42*, 475–485.

20. Fu, Y. W., Gao, J. M., Bieschke, J., Dendle, M. A., and Kelly, J. W. (2006) Amide-to-E-olefin versus amide-to-ester backbone H-bond perturbations: Evaluating the O-O repulsion for extracting H-bond energies. *J. Am. Chem. Soc. 128*, 15948–15949.

21. Bieschke, J., Siegel, S. J., Fu, Y. W., and Kelly, J. W. (2008) Alzheimer's A beta peptides containing an isostructural backbone mutation afford distinct aggregate morphologies but analogous cytotoxicity. Evidence for a common low-abundance toxic structure(s). *Biochemistry 47*, 50–59.

22. Soto, C., Sigurdsson, E. M., Morelli, L., Kumar, R. A., Castano, E. M., and Frangione, B. (1998) Beta-sheet breaker peptides inhibit fibrillogenesis in a rat brain model of amyloidosis: Implications for Alzheimer's therapy. *Nat. Med. 4*, 822–826.

23. Tanaka, M. (2007) Design and synthesis of chiral α,α-disubstituted amino acids and conformational study of their oligopeptides. *Chem. Pharm. Bull. (Tokyo) 55*, 349–358.

24. Ghanta, J., Shen, C.-L., Kiessling, L. L., and Murphy, R. M. (1996) A strategy for designing inhibitors of β-amyloid toxicity. *J. Biol. Chem. 271*, 29525–29528.

25. Etienne, M. A., Aucoin, J. P., Fu, Y. W., McCarley, R. L., and Hammer, R. P. (2006) Stoichiometric inhibition of amyloid beta-protein aggregation with peptides containing alternating alpha,alpha-disubstituted amino acids. *J. Am. Chem. Soc. 128*, 3522–3523.

26. Li, Q. Y., Gordon, M., Etienne, M. A., Hammer, R. P., and Morgan, D. (2008) Contrasting in vivo effects of two peptide-based amyloid-beta protein aggregation inhibitors in a transgenic mouse model of amyloid deposition. *Cell Transplant 17*, 397–408.

27. Bett, C. K., Ngunjiri, J. N., Serem, W. K., Fontenot, K. R., Hammer, R. P., McCarley, R. L., and Garno, J. C. (2010) Structure-activity relationships in peptide modulators of β-amyloid protein aggregation: Variation in alpha,alpha-disubstitution results in altered aggregate size and morphology, *ACS Chem. Neurosci.* [online early access], DOI: 10.1021/cn100045q.

28. Formaggio, F., Bettio, A., Moretto, V., Crisma, M., Toniolo, C., and Broxterman, Q. B. (2003) Disruption of the beta-sheet structure of a protected pentapeptide, related to the beta-amyloid sequence 17−21, induced by a single, helicogenic C-alpha-tetrasubstituted alpha-amino acid. *J. Pept. Sci. 9*, 461–466.

29. Gilead, S., and Gazit, E. (2004) Inhibition of amyloid fibril formation by peptide analogues modified with alpha-aminoisobutyric acid. *Angew. Chem., Int. Ed. 43*, 4041–4044.

30. Cairo, C. W., Strzelec, A., Murphy, R. M., and Kiessling, L. L. (2002) Affinity-Based Inhibition of beta-Amyloid Toxicity. *Biochemistry 41*, 8620–8629.

31. Austen, B. M., Paleologou, K. E., Ali, S. A. E., Qureshi, M. M., Allsop, D., and El-Agnaf, O. M. A. (2008) Designing peptide inhibitors for oligomerization and toxicity of Alzheimer's beta-amyloid peptide. *Biochemistry 47*, 1984–1992.

32. Li, Q., Gordon, M., Etienne Marcus, A., Hammer Robert, P., and Morgan, D. (2008) Contrasting in vivo effects of two peptide-based amyloid-beta protein aggregation inhibitors in a transgenic mouse model of amyloid deposition. *Cell Transplant 17*, 397–408.

33. Etienne, M. A., Aucoin, J. P., Fu, Y., McCarley, R. L., and Hammer, R. P. (2006) Stoichiometric inhibition of amyloid beta -protein aggregation with peptides containing alternating alpha, alpha-disubstituted amino acids. *J. Am. Chem. Soc. 128*, 3522–3523.

34. Krebs, M. R. H., Bromley, E. H. C., and Donald, A. M. (2005) The binding of thioflavin-T to amyloid fibrils: localisation and implications. *J. Struct. Biol. 149*, 30–37.

35. Levine, H. (1993) Thioflavine-T interaction with synthetic Alzheimers-disease beta-amyloid peptides: Detection of amyloid aggregation in solution. *Protein Sci. 2*, 404–410.

36. LeVine, H.III (1995) Thioflavine T interaction with amyloid beta-sheet structures. *Amyloid 2*, 1–6.

37. Nilsson, M. R. (2004) Techniques to study amyloid fibril formation in vitro. *Methods 34*, 151–160.

38. Lee, S., Fernandez, E. J., and Good, T. A. (2007) Role of aggregation conditions in structure, stability, and toxicity of intermediates in the A beta fibril formation pathway. *Protein Sci. 16*, 723–732.

39. Bieschke, J., Zhang, Q. H., Powers, E. T., Lerner, R. A., and Kelly, J. W. (2005) Oxidative metabolites accelerate Alzheimer's amyloidogenesis by a two-step mechanism, eliminating the requirement for nucleation. *Biochemistry 44*, 4977–4983.

40. Laczko, I., Vass, E., Soos, K., Fulop, L., Zarandi, M., and Penke, B. (2008) Aggregation of A beta(1−42) in the presence of short peptides: conformational studies. *J. Pept. Sci. 14*, 731–741.

41. Gazit, E. (2005) Mechanisms of amyloid fibril self-assembly and inhibition. *FEBS J. 272*, 5971–5978.

42. Wogulis, M., Wright, S., Cunningham, D., Chilcote, T., Powell, K., and Rydel, R. E. (2005) Nucleation-dependent polymerization is an essential component of amyloid-mediated neuronal cell death. *J. Neurosci. 25*, 1071–1080.

43. Kad, N. M., Myers, S. L., Smith, D. P., Smith, D. A., Radford, S. E., and Thomson, N. H. (2003) Hierarchical assembly of beta(2)-microglobulin amyloid in vitro revealed by atomic force microscopy. *J. Mol. Biol. 330*, 785–797.

44. Paravastu, A. K., Petkova, A. T., and Tycko, R. (2006) Polymorphic fibril formation by residues 10−40 of the Alzheimer's beta-amyloid peptide. *Biophys. J. 90*, 4618–4629.

45. Jarrett, J. T., Berger, E. P., and Lansbury, P. T. (1993) The carboxy terminus of the beta-amyloid protein is critical for the seeding of amyloid formation: Implications for the pathogenesis of Alzheimers-disease. *Biochemistry 32*, 4693–4697.

46. Soto, P., Griffin Mary, A., and Shea, J.-E. (2007) New insights into the mechanism of Alzheimer amyloid-beta fibrillogenesis inhibition by N-methylated peptides. *Biophys. J. 93*, 3015–3025.

47. Carulla, N., Caddy, G. L., Hall, D. R., Zurdo, J., Gairi, M., Feliz, M., Giralt, E., Robinson, C. V., and Dobson, C. M. (2005) Molecular recycling within amyloid fibrils. *Nature 436*, 554–558.

48. Fulop, L., Zarandi, M., Datki, Z., Soos, K., and Penke, B. (2004) beta-amyloid-derived pentapeptide RIIGL(a) inhibits A beta(1−42) aggregation and toxicity. *Biochem. Biophys. Res. Commun. 324*, 64–69.

49. El-Agnaf, O. M. A., Paleologou, K. E., Greer, B., Abogrein, A. M., King, J. E., Salem, S. A., Fullwood, N. J., Benson, F. E., Hewitt, R., Ford, K. J., Martin, F. L., Harriot, P., Cookson, M. R., and Allsop, D. (2004) A strategy for designing inhibitors of alpha-synuclein aggregation and toxicity as a novel treatment for Parkinson's disease and related disorders. *FASEB J. 18*, 1315–+.

50. Schmechel, A., Zentgraf, H., Scheuermann, S., Fritz, G., Pipkorn, R. D., Reed, J., Beyreuther, K., Bayer, T. A., and Multhaup, G. (2003) Alzheimer beta-amyloid homodimers facilitate A beta fibrillization and the generation of conformational antibodies. *J. Biol. Chem. 278*, 35317–35324.

51. Morimoto, A., Irie, K., Murakami, K., Masuda, Y., Ohigashi, H., Nagao, M., Fukuda, H., Shimizu, T., and Shirasawa, T. (2004) Analysis of the secondary structure of beta-amyloid (A beta 42) fibrils by systematic proline replacement. *J. Biol. Chem. 279*, 52781–52788.

52. Sato, T., Kienlen-Campard, P., Ahmed, M., Liu, W., Li, H. L., Elliott, J. I., Aimoto, S., Constantinescu, S. N., Octave, J. N., and Smith, S. O. (2006) Inhibitors of amyloid toxicity based on beta-sheet packing of A beta 40 and A beta 42. *Biochemistry 45*, 5503–5516.

53. O'Nuallain, B., Shivaprasad, S., Kheterpal, I., and Wetzel, R. (2005) Thermodynamics of abeta(1−40) amyloid fibril elongation. *Biochemistry 44*, 12709–12718.

54. Fu, Y. W., and Hammer, R. P. (2002) Efficient acylation of the N-terminus of highly hindered C-alpha,C-alpha-disubstituted amino acids via amino acid symmetrical anhydrides. *Org. Lett. 4*, 237–240.

55. Fu, Y. W., Hammarstrom, L. G. J., Miller, T. J., Fronczek, F. R., McLaughlin, M. L., and Hammer, R. P. (2001) Sterically hindered C-alpha,C-alpha-disubstituted alpha-amino acids: Synthesis from alpha-nitroacetate and incorporation into peptides. *J. Org. Chem. 66*, 7118–7124.

56. Fu, Y. W., Etienne, M. A., and Hammer, R. P. (2003) Facile synthesis of alpha,alpha-diisobutylglycine and anchoring its derivatives onto PAL-PEG-PS resin. *J. Org. Chem. 68*, 9854–9857.

57. Etienne, M. A., Edwin, N. J., Aucoin, J. P., Russo, P. S., McCarley, R. L., and Hammer, R. P. (2007) beta-Amyloid protein aggregation. *Methods Mol. Biol. 386*, 203–225.

DOI: 10.1021/cn900019r | *ACS Chem. Neurosci.* (2010), *1*, 661–678